Structure, Vol. 12, 593–602, April, 2004, ©2004 Elsevier Science Ltd. All rights reserved. DOI 10.1016/j.str.2004.03.003

Deep Knot Structure for Construction of Active Site and Cofactor Binding Site of tRNA Modification Enzyme

Osamu Nureki,[1,2,3,4,*] Kazunori Watanabe,[6] Shuya Fukai,[1] Ryohei Ishii,[3] Yaeta Endo,[6] Hiroyuki Hori,[6,*] and Shigeyuki Yokoyama[3,4,5]

[1]Department of Biological Information
Graduate School of Bioscience and Biotechnology
Tokyo Institute of Technology
4259 Nagatsuta-cho, Midori-ku
Yokohama-shi, Kanagawa 226-8501

[2]PRESTO, JST
4-1-8 Hon-cho
Kawaguchi-shi, Saitama 332-0012

[3]Department of Biophysics and Biochemistry
Graduate School of Science
University of Tokyo
7-3-1 Hongo
Bunkyo-ku, Tokyo 113-0033

[4]RIKEN Genomic Sciences Center
1-7-22 Suehiro-cho
Tsurumi, Yokohama 230-0045

[5]Cellular Signaling Laboratory
and Structurome Group
RIKEN Harima
Institute at SPring-8
1-1-1 Kouto Mikazuki-cho
Sayo-gun, Hyogo 679-5148

[6]Department of Biotechnology
Faculty of Engineering
Ehime University
Matsuyama 790-8577
Japan

Summary

The tRNA(Gm18) methyltransferase (TrmH) catalyzes the 2′-*O* methylation of guanosine 18 (Gua18) of tRNA. We solved the crystal structure of *Thermus thermophilus* TrmH complexed with S-adenosyl-L-methionine at 1.85 Å resolution. The catalytic domain contains a deep trefoil knot, which mutational analyses revealed to be crucial for the formation of the catalytic site and the cofactor binding pocket. The tRNA dihydrouridine(D)-arm can be docked onto the dimeric TrmH, so that the tRNA D-stem is clamped by the N- and C-terminal helices from one subunit while the Gua18 is modified by the other subunit. Arg41 from the other subunit enters the catalytic site and forms a hydrogen bond with a bound sulfate ion, an RNA main chain phosphate analog, thus activating its nucleophilic state. Based on Gua18 modeling onto the active site, we propose that once Gua18 binds, the phosphate group activates Arg41, which then deprotonates the 2′-OH group for methylation.

*Correspondence: onureki@bio.titech.ac.jp (O.N.), hori@eng.ehime-u.ac.jp (H.H.)

Introduction

Currently, two types of knots have been found in proteins: the trefoil knot, formed by threading a polypeptide chain through an untwisted loop, and the figure-of-eight knot, created by threading a polypeptide chain through a twisted loop (Taylor, 2000; Nureki et al., 2002). Trefoil knots exist in S-adenosylmethionine synthetase and carbonic anhydrase B (Takusagawa and Kamitori, 1996; Mansfield, 1997), but their knots are quite shallow and can disappear when viewed from a different angle. In contrast, the figure-of-eight knot is formed by a complicated process, e.g., domain swapping, in which a large domain passes through a long loop, which makes it difficult to identify the knot visually in the overall structure of the protein (Taylor, 2000). Actually, the first figure-of-eight knot, in plant acetohydroxy acid isomeroreductase, was discovered with a computer algorithm 3 years after the structure determination (Taylor, 2000).

Recently, we discovered a deep trefoil knot in the catalytic domain of *Thermus thermophilus* RrmA methyltransferase (MTase) (Nureki et al., 2002), a counterpart of *Escherichia coli* RlmB (described below). After our discovery, similar deep trefoil knots were found in three hypothetical RNA MTases (Michel et al., 2002; Zarembinski et al., 2003; Lim et al., 2003). In YibK from *Haemophilus influenzae*, the knot forms the binding crevice for S-adenosylhomocysteine (AdoHCys), which suggests that the protein is an MTase, although the substrate is unknown (Lim et al., 2003). On the other hand, genetic studies suggested that *E. coli* RlmB is involved in the 2′-*O* methylation of guanosine 2251 of 23S rRNA (Michel et al., 2002). All of the MTases contain the deep trefoil knot within the same catalytic fold, which has three common short amino acid motifs. Therefore, these hypothetical MTases were considered to form an enzyme family, named the "SpoU (tRNA [Gm18] methyltransferase) family" (Cavaillé et al., 1999). Recently, the tRNA(m^1G37)methyltransferase (TrmD) crystal structures from *H. influenzae*, *E. coli*, and *Aquifex aeolicus* were reported, and the TrmD structures contain a similar deep trefoil knot, except for that of *A. aeolicus* enzyme (Ahn et al., 2003; Elkins et al., 2003; Liu et al., 2003). TrmD has an N-terminal catalytic domain, with a topology similar to that of the SpoU MTase family, but it lacks the 3 amino acid motifs conserved in the SpoU family. Actually, it was previously predicted that the SpoU and TrmD MTase families share a common catalytic fold distinct from the "consensus MTase fold," and that the two families might thus share a common evolutionary origin and form a single "SpoU-TrmD (SPOUT)" class (Anantharaman et al., 2002). Extensive mutational analyses revealed the functional importance of the knotted structure in the *E. coli* TrmD enzyme (Elkins et al., 2003). In contrast, there are no in vitro data regarding the catalytic activity of the SpoU-family MTases, and thus the structure-function relationship of the conserved deep trefoil knot has remained elusive. Apart from the RNA MTases, the eukaryotic SET domain, involved in the

lysine methylation of the N-terminal tails of histones, has a deep trefoil knot within a different polypeptide fold, which was suggested to help form the MTase active site (Jacobs et al., 2002).

The tRNA (Gm18) MTase catalyzes the 2′-*O* methylation of guanosine at position 18 (Gua18) in the D loop of tRNA (Hori et al., 2002). The tRNA species from all organisms have Gua18, which forms a tertiary base pair with Ψ55 in the L-shaped tRNA core. The 2′-*O* methylation stabilizes the ribose C3′-endo puckering conformation to confer local conformational rigidity (Kawai et al., 1992), which may contribute to the stabilities of both the tRNA itself and the tRNA-protein interaction. An *E. coli* mutant with a *spoU* gene disruption lacked the Gm18 modification, thus identifying *spoU* was identified as encoding tRNA (Gm18) MTase (Persson et al., 1997). Therefore, the *spoU* gene was renamed *trmH* (tRNA methylation H) (Hori et al., 2002). However, no in vitro MTase activity has been detected for *E. coli* TrmH, as well as the TrmHs from various mesophilic bacteria and eukaryotes (type II TrmH) (Cavaillé et al., 1999; Persson et al., 1997). A type II TrmH, such as that from *Aquifex aeolicus*, was shown in vitro to methylate only restricted tRNA species (Hori et al., 2003). In contrast, TrmH from *Thermus thermophilus* exhibited MTase activity toward all tRNA species in vitro (type I TrmH) (Kumagai et al., 1980; Hori et al., 1998). An amino acid sequence alignment revealed that the type II TrmH has an extended C-terminal region, as compared with the type I enzyme, which may contribute to tRNA specificity (Hori et al., 2003). Using the type I *T. thermophilus* TrmH, the tRNA recognition mechanism was studied by RNA footprinting and RNA/protein fragmentation analyses (Hori et al., 2002; Matsumoto et al., 1990). These studies revealed that TrmH recognizes the tRNA D-arm structure, especially the nucleotides at positions 15, 17, 18, and 19, and this enzyme binding may weaken or break the D loop:TΨC loop interaction, resulting in a significant conformational change of the entire tRNA structure. For the TrmH protein, the N-terminal and/or C-terminal regions are indispensable for the tRNA recognition.

In the present study, we solved the crystal structure of *T. thermophilus* TrmH, the prototypical "SpoU family" MTase, complexed with S-adenosyl-L-methionine (AdoMet), at 1.85 Å resolution. In vitro methylation kinetics and cofactor binding analyses, based on the present structure, have now revealed the structure-function relationship of the conserved deep trefoil knot. The docking model with tRNA accounts well for the previous biochemical results, and suggests a novel RNA-dependent catalytic mechanism.

Results and Discussion

Overall Structure of *T. thermophilus* TrmH

TrmH (194 residues, M_r of 22,083) was crystallized in two distinct forms. The $P4_12_12$ form (form I) diffracts X-rays up to 2.0 Å resolution, and the *C*2 form (form II) diffracts beyond 1.85 Å resolution (Table 1). Both forms contain one TrmH molecule in the asymmetric unit. The current model at 1.85 Å resolution comprises residues 2–191 of TrmH, the tightly bound methyl donor cofactor S-adenosyl methionine (AdoMet), and a sulfate ion. The final 1.85 Å model has an R_{work} of 20.8% and an R_{free} of 25.5%, and shows very good geometry, as examined by a Ramachandran plot: 99.4% of the residues are observed in the most favored and additionally allowed regions (95.8% and 3.6%, respectively). The TrmH structure has a disc-like shape, composed of a major catalytic domain and a helical subdomain (Figure 1). The helical subdomain consists of the N-terminal helix α1 and the C-terminal helix α8, which interact with each other (Figure 1). The two helices have high B factors (average B factor of 37.4 Å^2), and in the $P4_12_12$ form (form I), they are partially disordered, which may account for the relatively high R factors at the higher resolutions. The flexibility of the helical subdomain is consistent with the previous biochemical results that the N- and C-terminal regions are susceptible to protease digestion and are essential for tRNA recognition (Hori et al., 2002).

The catalytic domain (residues 20–172) consists of a parallel six-stranded β sheet (β6-β4-β5-β1-β2-β3), which is flanked by two α helices (α4 and α6) on one side and by four α helices (α2, α3, α5, and α7) on the other side. The N-terminal half of the catalytic domain resembles a Rossmann fold or consensus MTase fold, while the C-terminal half has a different topology as compared with that of the consensus MTase fold: it includes a deep trefoil knot. The knot is formed by threading 55 amino acid residues (residues 140–194) through a hoop consisting of 12 residues (residues 97–108). The knotted polypeptide folds into α7 and α8, of which the latter forms the helical subdomain together with α1. The knot forms a deep crevice that accommodates AdoMet, as described below. Tyr97, Val111, Val119, and Phe121, from the hoop, and Ile140 and Ile160, from the thread, establish the hydrophobic core of the knot. The other hydrophobic core involves Leu101 from the hoop, Ile142, Met144, and Ile151 from the thread, and the adenine moiety of the bound AdoMet. The knot structure is further stabilized by a specific salt bridge between Glu103 from the hoop and Lys141 from the thread (Figure 1B), and by seven hydrogen bonds between the hoop and thread main chains (β4 and β6, respectively).

The TrmH catalytic domain can be superimposed onto those of *T. thermophilus* RrmA (Nureki et al., 2002), *E. coli* RlmB (Michel et al., 2002), and *H. influenzae* YibK (Lim et al., 2003), belonging to the same SpoU family, with rms deviations of 1.42 Å (128 Cαs), 1.34 Å (128 Cαs), and 1.07 Å (82 Cαs), respectively. The catalytic domain of TrmD (Ahn et al., 2003; Elkins et al., 2003; Liu et al., 2003) lacks one β strand as compared with those of the SpoU family enzymes, but the folding topology is the same. When we superimposed the catalytic domain of *H. influenzae* TrmD onto that of TrmH, the rmsd is 2.19 Å over 40 Cα carbons. Therefore, the SPOUT superfamily, formed by combining the SpoU and TrmD families, shares a characteristic catalytic fold with a deep trefoil knot, which is fundamentally different from that of the consensus MTase fold (Ahn et al., 2003; Elkins et al., 2003; Liu et al., 2003).

The Deep Trefoil Knot Forms the AdoMet Binding Pocket and the Active Site

The three sequence motifs that are highly conserved among the SpoU family MTases are located on β1-α2,

Table 1. Summary of Data Collection and Refinement Statistics

	SeMet L161M Crystal (Form I)				Native	+AdoMet
	Peak	Edge	Remote 1	Remote 2	(Form I)	(Form II)
Data collection						
Wavelength (Å)	0.9793	0.9795	0.9840	0.9723	0.9791	0.9000
Resolution (Å)	50–2.4	50–2.4	50–2.4	50–2.4	50–2.0	50–1.85
Unique reflections	7,883	7,894	7,791	8,012	13,450	13,887
Redundancy	10.3	10.1	10.0	9.9	10.5	3.3
Completeness (%)	98.4 (75.8)	98.4 (74.3)	96.4 (34.9)	99.3 (93.8)	99.1 (98.3)	98.0 (94.8)
$I/\sigma(I)$	8.8 (2.0)	8.4 (1.7)	8.1 (1.5)	8.4 (1.8)	13.4 (3.6)	12.4 (6.2)
R_{sym}[a](%)	8.8 (39.4)	8.9 (41.2)	8.7 (45.5)	8.9 (40.4)	5.8 (30.6)	4.4 (12.2)
Phasing Statistics						
No. of sites	3	3	3	3		
Phasing power						
Iso acent/cent	0.17/0.11	—	1.82/1.17	1.52/1.01		
R_{cullis}[b]						
Iso acent/cent	0.99/0.98	—	0.67/0.61	0.72/0.68		
Ano	0.50	0.69	0.95	0.51		
FOM acent/cent		0.75/0.60				
Refinement Statistics						
Resolution (Å)		50–2.5			50–2.1	50–1.85
Protein atoms		1,357			1,384	1,514
Substrate atoms		37			10	32
Water oxygens		189			213	94
R_{work}[c] (%)		25.8			24.7	20.8
R_{free}[d] (%)		30.2			29.5	25.5
Rmsd bond length (Å)		0.0184			0.0186	0.005
Rmsd bond angles (°)		1.64			2.04	1.30
Rmsd dihedrals (°)		23.4			24.4	22.1
Rmsd impropers (°)		0.94			1.12	1.29
Cross-validated sigma-A error (Å)		1.44			1.35	1.20

The numbers in parentheses are for the last shell.
[a] $R_{sym} = \Sigma|I_{avg} - I_i|/\Sigma I_i$.
[b] $R_{cullis} = \Sigma||F_{PH} + F_P| - F_H(calc)|/\Sigma|F_{PH}|$.
[c] $R_{work} = \Sigma|F_o - F_c|/\Sigma F_o$ for reflections of work set.
[d] $R_{free} = \Sigma|F_o - F_c|/\Sigma F_o$ for reflections of test set (10% of total reflections).

β5-α6, and β6-α7 (Figures 1A and 1C). The strictly conserved Asn35 in motif 1, Glu124 in motif 2, and Ser150 and Asn152 in motif 3 come in close proximity to each other, and form the putative catalytic site (Figure 2A). Actually, the side chain carboxyl group of Glu124 hydrogen bonds with the γ-amide group of Asn35 (2.91 Å), and the γ-carbonyl group of Asn35, in turn, hydrogen bonds with the γ-amide group of Asn152 (3.15 Å), thus forming a hydrogen-bonding network. Furthermore, the γ-amide groups of Asn35 and Asn152 form hydrogen bonds with the tightly bound sulfate ion (SO_4-1) (2.96 and 2.66 Å, respectively). Mutations of Glu124, Ser150, and Asn152 to Ala reduced the tRNA methylation activity by a magnitude of 5 (Table 2). Especially, Glu124 and Ser150/Asn152 are located on both sides of the knot 10–16 residues upstream and downstream, respectively, of the knotting point (Thr140) (see Nureki et al., 2002]) (Figure 2A). Therefore, the knot substructure is crucial for the catalytic site formation. Furthermore, the knotted loop, connecting β6 and α7, forms the edge of a deep crevice that accommodates the methyl-donor cofactor, AdoMet, which adopts an unusual, bent conformation (Figures 2A and 2B). Similar bent conformations of AdoMet or AdoHcy were observed in the complexes with *H. influenza* YibK (Lim et al., 2003), TrmD (Ahn et al., 2003; Elkins et al., 2003), and the *Drosophila* SET domain (Jacobs et al., 2002). The AdoMet is bound in the knot-forming L-shaped crevice, and projecting the donor methyl group toward the catalytic site of TrmH (Figures 2A and 2B). The adenine ring is surrounded by the hydrophobic side chains of Leu101, Ile142, Met144, Leu151, and Ala156, which provide van der Waals interactions with the base moiety within a distance of 4 Å (Figure 2B). Actually, the Ala substitutions of Leu101, Met144, and Leu151 increased the K_m value for AdoMet by 6- to 10-fold (Table 2). Furthermore, in analytical AdoHcy affinity column experiments, the M144A and L151A mutants exhibited weaker affinity to AdoHcy (Figure 2C). Leu101, Met144, and Leu151 are highly conserved in the SpoU family MTases (Figure 1C), suggesting that these hydrophobic residues are essential for recognition of the AdoMet adenine moiety. Two hydrogen-bonding interactions are observed, between the N6 group of the adenine base and the main chain carbonyl group of Ile142 (distance of 2.94 Å resolution), and between the N7 atom and the main chain amide group of Leu151 (distance of 2.92 Å resolution) (Figure 2B). These hydrogen-bonding interactions are also ob-

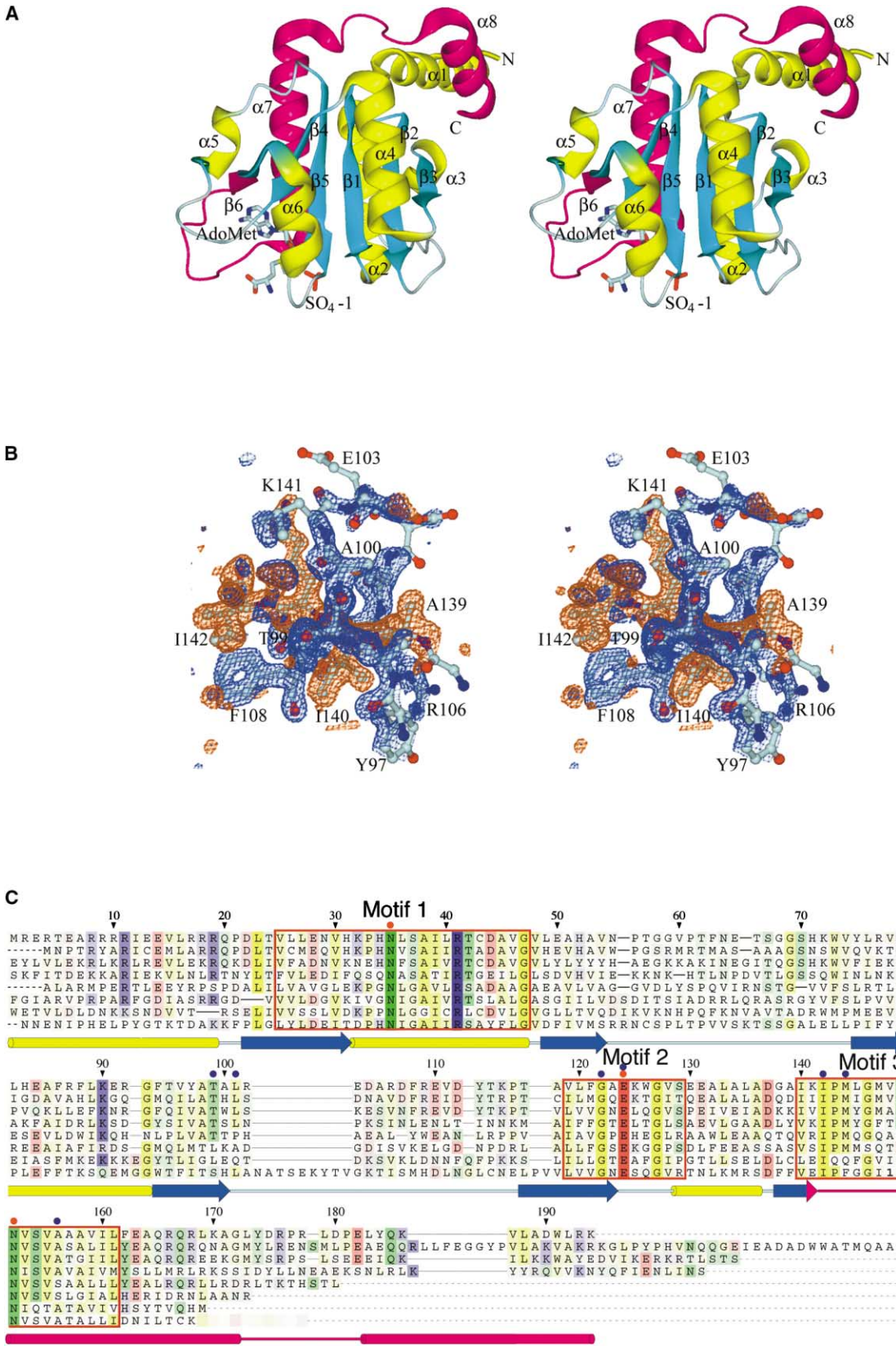

Figure 1. Crystal Structure of *T. thermophilus* TrmH

(A) A stereoview of the overall structure of *T. thermophilus* TrmH. The α helices are shown in yellow, the β strands are cyan, and the random coils are gray. The knotted polypeptide is magenta. All of the secondary structures are numbered. The bound cofactor, AdoMet, and the sulfate ion are shown.

served in the TrmD/AdoHCy complex (Ahn et al., 2003; Elkins et al., 2003). Therefore, the knotted loop (thread) constructs the adenine binding pocket. On the other hand, the 2′OH and 3′OH groups of the AdoMet ribose moiety form tight hydrogen bonds with the main chain amide group of Gly122 (2.58 Å) and the Oγ of Thr99 (2.62 Å), respectively (Figure 2B). However, the mutation of Thr99 to Ala reduced the methylation activity by only 3-fold. The terminal carboxyl and amino groups of the AdoMet methionine moiety lack specific interactions with the protein (Figure 2B), and show high B factors, as also observed in *E. coli* TrmD (Elkins et al., 2003). The donor methyl group of AdoMet provides van der Waals interactions with the Cα atom of Glu124 at a distance of 3.84 Å (Figure 2B). Glu124 is anchored by hydrogen-bonding interactions between the side chain carboxyl group and the main chain amide groups of His31 and Lys32 (data not shown). Thus, the peptide segment encompassing Gly122–Glu124 forms a platform that holds the ribose and methionine moieties of AdoMet to facilitate the bent, active conformation (Figure 2B), which may account for the significantly high K_m value (2800-fold) for AdoMet in the E124A mutant. In *E. coli* TrmD, Ala-scanning mutations of the corresponding region (SpoU motif II) inactivated the enzyme, suggesting that the region is critical for the maintenance of the knot or adenine binding loop conformation as well as for the dimer interface formation (Elkins et al., 2003). Therefore, the deep knot structure of TrmH is crucial for the construction of the AdoMet binding site as well as the active site, as also discussed for *E. coli* TrmD (Elkins et al., 2003).

The structures of the AdoMet/AdoHcy binding pocket and the active site are quite similar between TrmH and *H. influenza* YibK, which belong to the same SpoU family, while the catalytic, substrate-recognizing loop encompassing residues 146–151 (TrmH numbering) is structurally disordered in YibK (Lim et al., 2003). In the *Drosophila* SET 7/9 domain, AdoHcy is recognized in a quite similar bent conformation, but the cofactor binding pocket is formed by residues from the hoop (Jacobs et al., 2002), whereas in the present TrmH structure, the AdoMet binding pocket is formed mainly by residues from the thread.

Among the three TrmH structures solved here, the SeMet crystal ($P4_12_12$ [form I]; 2.5 Å resolution) and the $C2$ form crystal (form II) (1.85 Å resolution) represent the complex with AdoMet, while the native crystal ($P4_12_12$ [form I]; 2.0 Å resolution) represents the apo form. When we compared the structures of the AdoMet complex and apo forms, the AdoMet binding crevice became narrower upon cofactor binding, involving the movement of two loops encompassing residues 124–128 and 142–151. Therefore, an induced-fit conformational change occurs upon cofactor binding. It was also previously discussed that the knotted methyltransferases may undergo isomerization during catalysis, in order to cycle AdoMet in and out of the deep cofactor binding pocket (Elkins et al., 2003).

Molecular Dimerization Is Essential for tRNA Recognition and Catalysis by TrmH

While the asymmetric unit of the crystals contains only one molecule, TrmH has extensive interactions with a symmetry-related molecule. The buried surface area in the dimer interface is 1,353 Å^2, which is 14% of the total surface area per monomer (9,700 Å^2). The TrmH sedimentation equilibrium experiment yielded a molecular weight of 48,000 (data not shown). These results strongly suggest that the TrmH protein behaves as an α_2 dimer under the experimental conditions. In the crystal structure, the 2-fold axis is almost parallel to the knotted helix α7. The dimer formation involves a hydrophobic interaction between Val159 and Phe162′ ("′" denotes a residue from the other subunit), and a hydrogen bond between Arg109 (η-amino group) and Gln165′ (γ-carbonyl group) (data not shown). All of these residues are derived from the two symmetry-related α7 helices. Furthermore, the protruding knotted loop connecting β6 and α7 contacts the catalytic core domain from the other subunit; the side chain of Met147 provides hydrophobic interactions with Ile12′ (α1) and Trp73′ (α3), the main chain carbonyl group of Met147 hydrogen bonds with the η-amino group of Arg11′ (α1), and Leu145 has a hydrophobic interaction with Tyr174′ (α8). These results suggest that the knot structure of TrmH also has a role in molecular dimerization, as previously described for SpoU family enzymes (Michel et al., 2002; Zarembinski et al., 2003; Lim et al., 2003). In TrmD, the trefoil knot structure facilitates the molecular dimerization (Ahn et al., 2003). However, it should be noted that SpoU family members form dimers in a parallel fashion, while the TrmD dimer is antiparallel, as described previously (Ahn et al., 2003).

The previous tRNA footprinting and kinetic experiments showed that *T. thermophilus* TrmH recognizes the tRNA D-arm, especially Gua15, Uri(D)17, Gua18, and Gua19, leading to deformation of the acceptor-stem-TΨC-arm helix (Matsumoto et al., 1990). Limited proteolysis produced the TrmH core domain, encompassing Ile12 to Arg168, which retained the SAH binding activity but lacked the tRNA methylation activity (Hori et al., 2002). This strongly suggests that the helical subdomain consisting of the N-terminal and C-terminal helices, α1

(B) An omit $F_o - F_c$ map contoured at 3.0 σ for the knot region. The electron density map for the "hoop" (residues 97–108) is colored blue, and that for the "thread" (residues 139–142) is red.

(C) Sequence alignment of the TrmHs from various organisms and of the homologous SpoU family MTases. Abbreviations are as follows: Tt, *T. thermophilus*; Ec, *E. coli*; Aq, *Aquifex aeolicus*; Bb, *Borrelia burgdorferi*; Sa, *Streptomyces azureus*; Sc, *Saccharomyces cerevisiae*. Secondary structural elements of *T. thermophilus* TrmH are shown below the alignment, with color codes as in Figure 1A. Insertions are denoted with the number of inserted residues. Identical amino acids and conservative replacements are colored in dark and light orange, respectively. Conserved acidic, neutral, basic, and hydrophobic residues are colored red, green, blue, and yellow, respectively. The three conserved motifs, 1, 2, and 3, are indicated with red boxes. The amino acid residues essential for catalysis and AdoMet binding are marked with red and blue circles, respectively, above the alignment.

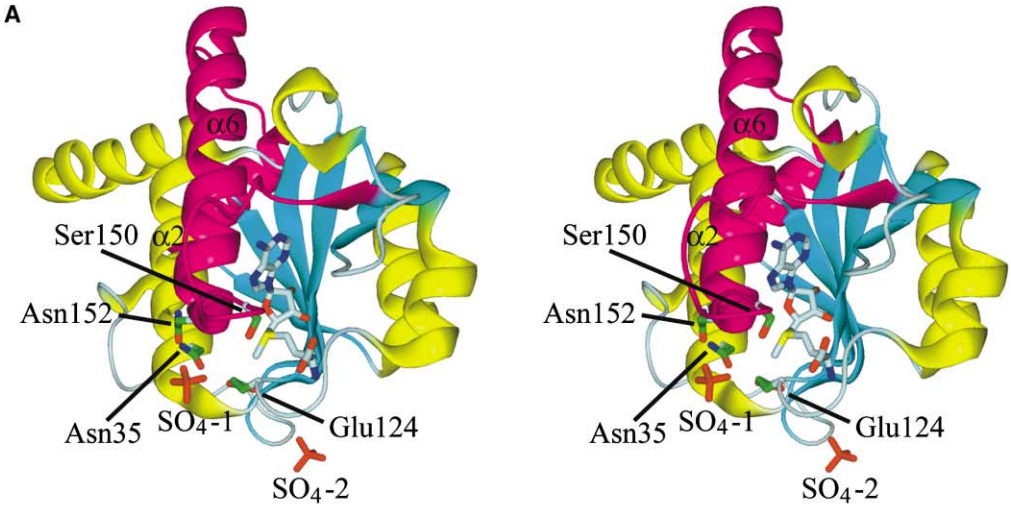
A
α6
Ser150
α2
Asn152
Asn35
SO4-1
Glu124
SO4-2
α6
Ser150
α2
Asn152
Asn35
SO4-1
Glu124
SO4-2

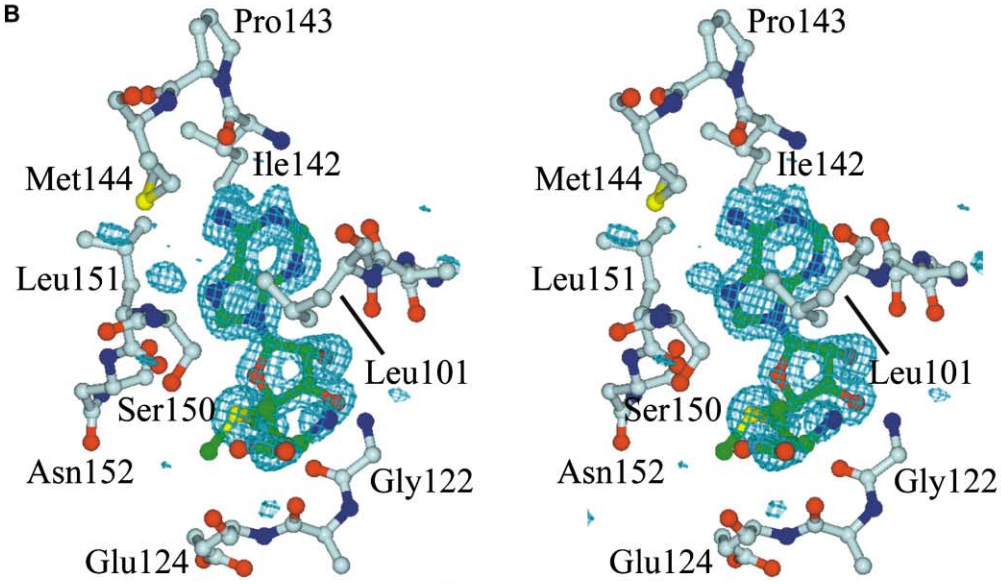
B
Pro143
Met144
Ile142
Leu151
Leu101
Ser150
Asn152
Gly122
Glu124
Pro143
Met144
Ile142
Leu151
Leu101
Ser150
Asn152
Gly122
Glu124

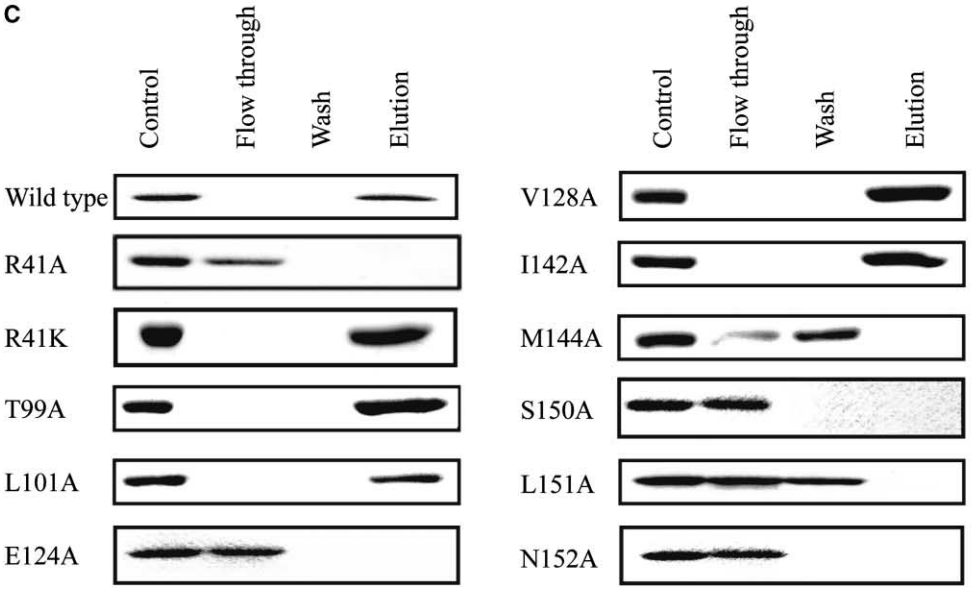
C
Control
Flow through
Wash
Elution
Wild type
R41A
R41K
T99A
L101A
E124A
Control
Flow through
Wash
Elution
V128A
I142A
M144A
S150A
L151A
N152A

Table 2. Kinetic Parameters of TrmH Mutants

Mutant	K_m for AdoMet (μM)	V_{max} (μmol/mg·h)	Relative V_{max}/K_m
Wild type	10	10	1
R41A	ND	ND	ND
R41K	300	0.41	0.0030
T99A	17	5.4	0.32
L101A	130	1.6	0.012
V128A	14	4.1	0.29
E124A	28000	0.46	0.000016
I142A	10	4.9	0.49
M144A	150	1.3	0.0087
S150A	1700	0.066	0.000039
L151A	56	0.55	0.0098
N152A	800	0.04	0.000050

ND, not detectable.

and α8, encompassing residues 1–20 and 183–194, respectively, is crucial for the tRNA recognition. However, in the present structure, the catalytic site and the helical subdomain are located at the two opposite ends within one TrmH molecule. We docked a tRNA D-arm onto the TrmH dimer, in which the tRNA D-stem is clamped by the α1 and α8 helices from one subunit, and Gua18 closely approaches the catalytic site of the other subunit, thus binding the tRNA across the TrmH dimer (Figure 3). It is likely that Gua18 flips out and binds to the catalytic site pocket (see below in Figure 4). However, when we docked the whole tRNA molecule, based on the docked tRNA D-arm, the tRNA main body seriously clashed with the catalytic domain of one TrmH molecule (Figure 3). This result suggests that upon binding to TrmH, the tRNA undergoes a significant conformational change that disrupts the D loop:TΨC loop interactions, as recently observed in another tRNA modification enzyme that modifies the tRNA core region (Ishitani et al., 2003).

Considering the active site of one TrmH subunit, Arg41′ from the other subunit enters into the catalytic site, and forms hydrogen bonds with the tightly bound sulfate ion (SO_4-1) (3.47 Å) and with the side chain hydroxyl group of Ser150 (2.84 Å) (Figure 4). Furthermore, the main chain carbonyl group of Ser150 hydrogen bonds with the guanidine group of Arg41′ (2.65 Å) (Figure 4). These interactions may withdraw a proton(s) from the side chain of Arg41′, thus converting the terminal amino group(s) to the nucleophilic state to act as a catalytic base. Arg41 is strictly conserved in all of the SpoU family members (motif 1 in Figure 1C), and is likely to function as a catalytic nucleophile, as described below. Actually, the mutation of Arg41 to Ala abolished the methylation activity (Table 2), and eliminated the affinity to AdoHCy in the analytical AdoHCy affinity column chromatography (Figure 2C). Therefore, the molecular dimerization of TrmH, which is facilitated by the deep trefoil knot structure, is critical not only for tRNA recognition but also for methylation catalysis itself. A similar situation was observed and discussed for *E. coli* TrmD enzyme (Elkins et al., 2003).

Novel RNA-Dependent Methylation Mechanism

The present structure revealed that a sulfate ion is tightly bound to the TrmH molecule (Figure 1A). Considering the fact that a sulfate ion is regarded as an analog of a phosphate group in an RNA main chain, Gua18 of tRNA was modeled onto the active site, to allow the sulfate ion, SO_4-1, to mimic the 5′ phosphate group (Figure 4). To model Gua18 onto this position, the nucleoside should be rotated on its sugar-phosphate backbone so that the base projects out into the catalytic pocket. Such "base-flipping" mechanisms are observed in a number of nucleic acid methyltransferases as well as some tRNA modification enzymes (Cheng and Roberts, 2001; Hoang and Ferre-D'Amare, 2001; Xie et al., 2003). The space surrounded by SO_4-1, AdoMet, and catalytically important residues, such as Ser150, Arg41′, Asn35, Glu124, and Asn152, is occupied by four tightly bound water molecules (data not shown), onto which Gua18 was modeled without any serious clashes with TrmH. One of the four water molecules is located within 2.94 Å from the η-amino group of Arg41′ (Figure 4), onto which the 2′-OH group of Gua18 could be modeled. Thus, we can envision a novel catalytic mechanism for TrmH: once Gua18 binds to the active site pocket, the 5′ phosphate group, which is tetrahedrally recognized by Lys32 (2.45 Å), His34 (2.81 Å), Asn35 (2.96 Å), and Asn152 (2.66 Å) (Figure 4), may withdraw a proton from the η-amino group of Arg41′, as described above. Since the second η-amino group of Arg41′ is also converted into the nucleophilic state by Ser150 (Figure 4), it may act as a catalytic base and deprotonate the 2′-OH group of Gua18. Thus, the activated 2′-OH group may then make a direct nucleophilic attack on the reactive methyl group of AdoMet (Figure 4). Therefore, it is likely that the methylation of Gua18 is triggered by its 5′ phosphate group, representing a novel RNA-dependent reaction mechanism. Based on the present hypothesis, Lys probably cannot substitute for Arg41 without reducing the catalytic activity, due to the differences in the side chain lengths and the number of functional groups (Figure 4). Actually, the mutation of Arg41 to Lys significantly reduced the methylation activity, by almost three orders of magnitude (Table 2). Intriguingly, in RrmA, belonging to the same SpoU family, the orientations of all of the catalytic residues are the same as those in TrmH (Nureki et al., 2002), and a strong electron density, which may represent a sulfate ion from the crystallization material, exists near the corresponding Arg residue (Arg135) (data

Figure 2. AdoMet Binding of TrmH

(A) A stereoview of the TrmH structure, highlighting the knot, active site, and AdoMet binding. The catalytically important residues, the tightly bound AdoMet, and the sulfate ions are indicated. The color codes are the same as in Figure 1A.

(B) Stereoview of the AdoMet binding site and the bound cofactor. The simulated omit $F_o - F_c$ map for AdoMet, contoured at 4.0 σ, is shown.

(C) Analytical AdoHCys affinity column chromatography of TrmH mutants. Experimental procedures are shown in the Experimental Procedures section.

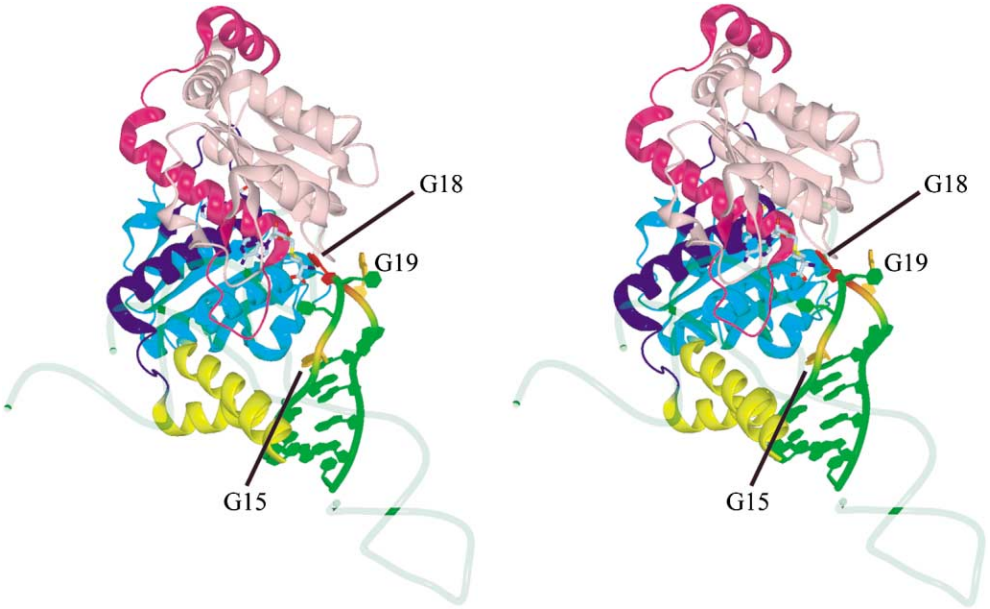

Figure 3. Docking Model of the tRNA D-Arm and the TrmH Dimer

Each subunit of the TrmH dimer is colored pink or cyan, with the knotted polypeptide magenta or blue, respectively. The tRNA D-arm is shown in green, with the recognized G15, G18, and G19 indicated. The helical subdomain of one monomer recognizing the tRNA D-stem is colored in yellow. The whole tRNA structure, transparently shown in green, has serious clashes with the catalytic domain of one monomer.

not shown). Therefore, the RNA-dependent methylation mechanism is likely to be common to all of the SpoU family MTases. It should be noted that, in the evolutionally related TrmD, the catalytic base was suggested to be an Asp residue derived from the other subunit of the dimer (Ahn et al., 2003; Elkins et al., 2003). This indicates that, in the SPOUT family MTases, the two subunits of the dimer cooperatively form the catalytic site.

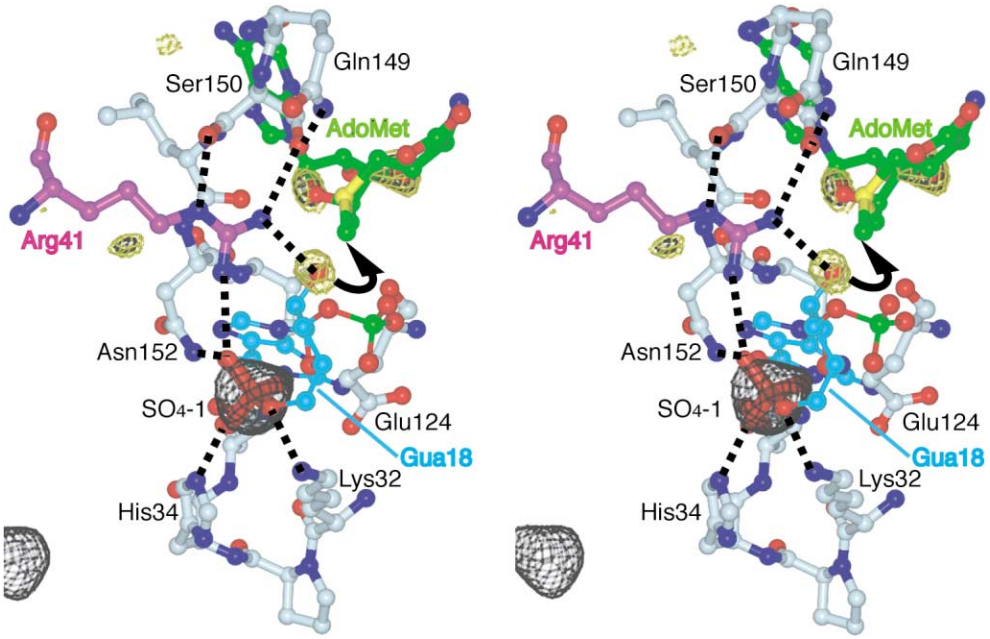

Figure 4. The RNA-Dependent Catalytic Mechanism

The simulated omit $F_o - F_c$ maps for the tightly bound sulfate ion and the water molecule, contoured at 4.0 σ, are shown. The bound AdoMet cofactor is shown in green. Based on the sulfate ion (phosphate group analog) and the water molecule, Gua18 is modeled onto the active site pocket. Arg41 from the other subunit of the dimer, indicated in purple, might act as a catalytic base that withdraws a proton from the 2′-OH group of Gua18 and allows it to attack the methyl group of AdoMet. Possible hydrogen bonds are indicated with dotted lines.

Experimental Procedures

Purification of Proteins

The wild-type and mutant enzyme were purified according to the previously reported method (Hori et al., 2002). Since four mutant proteins (M144A, S150A, L151A, and N152A) did not bind to the AdoHCys affinity column, we purified these proteins by repeated steps of ion exchange chromatography. The pooled fractions from DE52 column chromatography were combined, dialyzed against buffer (50 mM HEPES-NaOH [pH 6.8], 5 mM $MgCl_2$, and 6 mM 2-mercaptoethanol), and loaded onto a CM-Toyopearl 650 M column. A linear gradient was developed from 0 to 300 mM KCl. The fractions enriched for the mutant enzyme were combined, dialyzed against buffer (50 mM Tris-HCl [pH 7.5], 5 mM $MgCl_2$, 2 mM mercaptoethanol, and 50 mM KCl), and concentrated with Centriprep YM-10 centrifugal filters (Millipore).

Measurements of the Enzymatic Activities

The standard assay for the enzyme purification was carried out by measuring methyl group incorporation from [Methyl-^{14}C]-AdoMet into the yeast tRNA^{Phe} transcript. Briefly, 300 ng protein, 7 μM transcript, and 38 μM [Methyl-^{14}C]-AdoMet, in 30 μl of buffer (50 mM Tris-HCl [pH 7.6], 5 mM $MgCl_2$, 6 mM 2-mercaptoethanol, and 50 mM KCl), were incubated for 5 min at 50°C. An aliquot (20 μl) was used for the conventional filter assay. The apparent kinetic parameters, K_m and V_{max}, were determined by a Lineweaver-Burk plot of the methyl-transfer reaction with [Methyl-^{14}C]-AdoMet or [Methyl-^{3}H]-AdoMet. When the activity of the mutant protein was low, [Methyl-^{3}H]-AdoMet diluted with cold AdoMet was used. The concentrations of the mutant proteins and the yeast tRNA^{Phe} transcript were fixed to 0.23 μM and 8.5 μM, respectively; however, the AdoMet concentrations and the incubation times were changed according to the methyl-transfer activity. When testing mutant proteins with relatively high activity, the [Methyl-^{14}C]-AdoMet concentrations were 0–30 μM. For the mutant proteins with relatively low activity, the [Methyl-^{3}H]-AdoMet concentrations were 0–2.0 mM.

Analytical AdoHCys Affinity Column Chromatography

The affinity of the purified proteins for AdoHCys was qualitatively analyzed by the AdoHCys affinity column chromatography. The sample (50 μg) was applied to the column (1 ml), which was washed with 5 ml of buffer (50 mM Tris-HCl [pH 7.6], 5 mM $MgCl_2$, 6 mM 2-mercaptoethanol, and 50 mM KCl). The flowthrough and buffer-washed fractions were combined and named the "flowthrough" fraction. Then, the column was washed with 5 ml of buffer containing 2 M KCl, and this fraction was named the "wash" fraction. Finally, the bound protein was eluted with 5 ml of buffer containing 2 M KCl and 6 M urea, and this fraction was named the "elution" fraction. The protein was precipitated from 300 μl of each fraction, by the addition of 100% trichloroacetic acid (Nacalai Tesque, Japan) to a final concentration of 5%, collected by centrifugation, dissolved in 10 μl of 1 M Tris-HCl (pH 8.0), and analyzed by 15% SDS-PAGE.

Crystallizations

Screenings of the crystallization conditions for the wild-type enzyme (10.0 mg/ml) were carried out at 4°C, 20°C, and 25°C by the hanging-drop vapor-diffusion method. Excellent crystal growth (form I) was observed at 20°C in 0.1 M Tris-HCl buffer (pH 8.5) containing 0.2M lithium sulfate monohydrate and 15% polyethylene glycol 4000. The crystals of the selenomethionyl protein appeared under similar conditions at 4°C. The form I crystals belong to the tetragonal space group ($P4_12_12$: a = b = 43.86 Å, c = 193.0 Å). After the structural determination of the form I crystals, the second crystal form (form II) appeared at 20°C in 50 mM Tris-HCl buffer (pH 8.5) containing 25 mM $MgSO_4$ and 1.8 M ammonium sulfate. The form II crystals belong to the monoclinic space group ($C2$: a = 77.60 Å, b = 44.02 Å, c = 56.76 Å, and β = 120.8°). To collect the data under flash-freezing conditions, the form I and II crystals were stabilized in harvest buffer, with 1.1-fold concentrations of reservoir solutions, including 15% ethylene glycol in both cases. The complex with AdoMet was prepared by soaking the crystals in harvest buffer containing 10 mM AdoMet for 4 hr.

Structure Determination and Refinement

Selenomethione-labeled TrmH was prepared according to the standard protocol (Doublié, 1997). MAD data from selenomethionine-labeled form I crystals (AdoMet complex) were collected at beamline BL41XU in SPring-8 (Harima) to 2.5 Å resolution. The data were processed and scaled with HKL2000 (Otwinowski and Minor, 1997). Three selenium sites were found by the direct method, using the Shake-and-Bake program (Weeks and Miller, 1999). The selenium parameters were refined and the phases were calculated using SHARP (de La Fortelle and Bricogne, 1997). Phases were improved by density modification using SOLOMON (Abrahams and Leslie, 1996). However, the resultant map lacked sufficient quality to trace the entire backbone. Therefore, we mutated Leu161 of TrmH to Met, to incorporate a new Met residue, and prepared the selenomethionine-labeled mutant. MAD phasing using crystals of this mutant enabled us to unambiguously trace the backbone from residues 12 to 65 and 70 to 191. An atomic model was fitted into the electron density map, using the graphics program O (Jones et al., 1991). Crystallographic positional and simulated annealing refinements were carried out against the 2.5 Å data set of the AdoMet complex and the 2.0 Å data set of the native crystals using CNS (Brünger et al., 1998). The form II crystals of the AdoMet complex diffracted X-rays beyond 1.5 Å resolution at beamline BL41XU in SPring-8 (Harima). The phases of the form II crystals were determined by molecular replacement, using the crystal structure of the form I crystal as a search model, with the program AMORE (CCP4, 1994). The excellent quality of the resulting electron density map allowed us to trace residues 2–190. The phasing and refinement statistics are summarized in Table 1.

Acknowledgments

This work was supported by a PRESTO Program grant from JST (Japan Science and Technology) to O.N., a Naito Foundation grant to O.N., and by Grants-in-Aid for Science Research on Priority Areas (15032209) to O.N. and Grants-in-Aid for Science Research (13680692) to H.H., from the Ministry of Education, Culture, Sports, Science, and Technology of Japan. This work was also supported by the RIKEN Structural Genomics/Proteomics Initiative (RSGI), the National Project on Protein Structural and Functional Analyses, Ministry of Education, Culture, Sports, Science, and Technology of Japan. We are greatly indebted to Drs. M. Kawamoto and H. Sakai (JASRI) for their help in data collection at SPring-8.

Received: November 4, 2003
Revised: January 20, 2004
Accepted: January 28, 2004
Published: April 6, 2004

References

Abrahams, J.P., and Leslie, A.G.W. (1996). Methods used in the structure determination of bovine mitochondrial F1 ATPase. Acta Crystallogr. D *52*, 30–42.

Ahn, H.J., Kim, H.-W., Yoon, H.-J., Lee, B.I., Suh, S.W., and Yang, J.K. (2003). Crystal structure of tRNA(m^{1}G37)methyltransferase: insights into tRNA recognition. EMBO J. *22*, 2593–2603.

Anantharaman, V., Koonin, E.V., and Aravind, L. (2002). SPOUT: a class of methyltransferases that includes spoU and trmD RNA methylase superfamilies and novel superfamilies of predicted prokaryotic RNA methylases. J. Mol. Microbiol. Biotechnol. *4*, 71–75.

Brünger, A.T., Adams, P.D., Clore, G.M., DeLano, W.L., Gros, P., Grosse-Kunstleve, R.W., Jiang, J.S., Kuszewski, J., Nilges, M., Pannu, N.S., et al (1998). Crystallography & NMR system: a new software suite for macromolecular structure determination. Acta Crystallogr. D *54*, 905–921.

Cavaillé, J., Chetouani, F., and Bachellerie, J.-P. (1999). The yeast Saccharomyces cerevisiae YDL112w ORF encodes the putative 2′-O-ribose methyltransferase catalyzing the formation of Gm18 in tRNAs. RNA *5*, 66–81.

Cheng, X., and Roberts, R. (2001). AdoMet-dependent methylation,

DNA methyltransferases and base flipping. Nucleic Acids Res. *29*, 3784–3795.

CCP4 (Collaborative Computational Project 4) (1994). The CCP4 suite: programs for protein crystallography. Acta Crystallogr. D *50*, 760–763.

de La Fortelle, E., and Bricogne, G. (1997). Maximum-likelihood heavy-atom parameter refinement for multiple isomorphous replacement and multiwavelength anomalous diffraction methods. Methods Enzymol. *276*, 472–494.

Doublié, S. (1997). Preparation of selenomethionyl proteins for phase determination. Methods Enzymol. *276*, 523–530.

Elkins, P.A., Watts, J.M., Zalacain, M., van Thiel, A., Vitazka, P.R., Redlak, M., Andraos-Selim, C., Rastinejad, F., and Holmes, W.M. (2003). Insights into catalysis by a knotted TrmD tRNA methyltransferase. J. Mol. Biol. *333*, 931–949.

Hoang, C., and Ferre-D'Amare, A. (2001). Cocrystal structure of a tRNA Ψ55 pseudouridine synthetase: nucleotide flipping by an RNA-modification enzyme. Cell *107*, 929–939.

Hori, H., Yamazaki, N., Matsumoto, T., Watanabe, Y., Ueda, T., Nishikawa, K., Kumagai, I., and Watanabe, K. (1998). Substrate recognition of tRNA(guanosine-2′-)-methyltransferase from *Thermus thermophilus* HB27. J. Biol. Chem. *273*, 25721–25727.

Hori, H., Suzuki, T., Sugawara, K., Inoue, Y., Shibata, T., Kuramitsu, S., Yokoyama, S., Oshima, T., and Watanabe, K. (2002). Identification and characterization of tRNA(Gm18)methyltransferase from *Thermus thermophilus* HB8: domain structure and conserved amino acid sequence motifs. Genes Cells *7*, 259–272.

Hori, H., Kubota, S., Watanabe, K., Kim, J.M., Ogasawara, T., Sawasaki, T., and Endo, Y. (2003). Aquifex aeolicus tRNA (Gm18) methyltransferase has unique substrate specificity. tRNA recognition mechanism of the enzyme. J. Biol. Chem. *278*, 25081–25090.

Ishitani, R., Nureki, O., Nameki, N., Okada, N., Nishimura, S., and Yokoyama, S. (2003). Alternative tertiary structure of tRNA for recognition by a posttranscriptional modification enzyme. Cell *113*, 383–394.

Jacobs, S.A., Harp, J.M., Devarakonda, S., Kim, Y., Rastinejad, F., and Khorasanizadeh, S. (2002). The active site of the SET domain is constructed on a knot. Nat. Struct. Biol. *9*, 833–838.

Jones, T.A., Zou, J.-Y., Cowan, S.W., and Kjeldgaard, M. (1991). Improved methods for building protein models in electron density maps and the location of errors in these models. Acta Crystallogr. A *47*, 110–119.

Kawai, G., Yamamoto, Y., Kamimura, T., Sekine, M., Hata, T., Iimori, T., Watanabe, T., Miyazawa, T., and Yokoyama, S. (1992). Conformational rigidity of specific pyrimidine residues in tRNA arises from posttranscriptional modifications that enhance steric interaction between the base and the 2′-hydroxyl group. Biochemistry *31*, 1040–1046.

Kumagai, I., Watanabe, K., and Oshima, T. (1980). Thermally induced biosynthesis of 2′-O-methylguanosine in tRNA from an extreme thermophile, *Thermus thermophilus* HB27. Proc. Natl. Acad. Sci. USA *77*, 1922–1926.

Lim, K., Zhang, H., Tempczyk, A., Krajewski, W., Bonander, N., Toedt, J., Howard, A., Eisenstein, E., and Herzberg, O. (2003). Structure of the YibK methyltransferase from *Haemophilus influenza* (HI0766): a cofactor bound at a site formed by a knot. Proteins *51*, 56–67.

Liu, J., Wang, W., Shin, D.H., Yokota, H., Kim, R., and Kim, S.-H. (2003). Crystal structure of tRNA(m^1G37)methyltransferase from *Aquifex aeolicus* at 2.6 Å resolution: a novel methyltransferase fold. Proteins *53*, 326–328.

Mansfield, M.L. (1997). Fit to be tied. Nat. Struct. Biol. *4*, 166–167.

Matsumoto, T., Nishikawa, K., Hori, H., Ohta, T., Miura, K., and Watanabe, K. (1990). Recognition sites of tRNA by a thermostable tRNA (guanosine-2′-)-methyltransferase from *Thermus thermophilus* HB27. J. Biochem. (Tokyo) *107*, 331–338.

Michel, G., Sauvé, V., Larocque, R., Li, Y., Matte, A., and Cygler, M. (2002). The structure of the RmlB 23S rRNA methyltransferase reveals a new methyltransferase fold with a unique knot. Structure *10*, 1303–1315.

Nureki, O., Shirouzu, M., Hashimoto, K., Ishitani, R., Terada, T., Tamakoshi, M., Oshima, T., Chijimatsu, M., Takio, K., Vassylyev, D.G., et al. (2002). An enzyme with a deep trefoil knot for the active-site architecture. Acta Crystallogr. D *58*, 1129–1137.

Otwinowski, Z., and Minor, W. (1997). Processing of X-ray diffraction data collected in oscillation mode. Methods Enzymol. *276*, 307–326.

Persson, B.C., Jager, G., and Gustaffson, C. (1997). The *spoU* gene of *Escherichia coli*, the fourth gene of the *spoT* operon, is essential for (Gm18) 2′-O-methyltransferase activity. Nucleic Acids Res. *25*, 3969–3973.

Takusagawa, F., and Kamitori, K. (1996). A real knot in protein. J. Am. Chem. Soc. *118*, 8945–8946.

Taylor, W.R. (2000). A deeply knotted protein structure and how it might fold. Nature *406*, 916–919.

Weeks, C.M., and Miller, R. (1999). The design and implementation of SnB version 2.0. J. Appl. Crystallogr. *32*, 120–124.

Xie, W., Liu, X., and Huang, R.H. (2003). Chemical trapping and crystal structure of a catalytic tRNA guanine transglycosylase covalent intermediate. Nat. Struct. Biol. *10*, 781–788.

Zarembinski, T.I., Kim, Y., Peterson, K., Christendat, D., Dharamsi, A., Arrowsmith, C.H., Edwards, A.M., and Joachimiak, A. (2003). Deep trefoil knot implicated in RNA binding found in an archaebacterial protein. Proteins *50*, 177–183.

Accession Numbers

The coordinates and structure factors have been deposited in the Protein Data Bank (accession code 1V2X).